

Short Note

On Scaling of Earthquake Rise-Time Estimates

by Alexander A. Gusev^{*†} and Danila Chebrov

Abstract The scaling behavior of rise times T_r determined within earthquake source inversions that used strong-motion data is determined using estimates as accumulated in the SRCMOD database. The T_r versus M_0 trend derived from this data set is close to $\log T_r = 1/3 \log M_0 + \text{const}$; this agrees with the assumption of self-similarity of earthquake ruptures. No biasing effect of station distance on T_r was found. The result was compared to recent scaling estimates based on mass teleseismic inversions. Absolute levels of teleseismic and local inversions match well; the slope of the trend of teleseismic estimates is somewhat more gradual. The absolute levels of T_r versus M_0 trends recovered from finite source inversions may need reduction when used to predict parameters of near-source ground motion. The observed scaling behavior of T_r is incompatible with the assumption that T_r defines the second corner frequency of the source spectrum.

Introduction

Properties of rise time T_r of earthquake rupture, that is, slip duration at a point of a fault, are interesting for the physics of earthquake sources and important for strong-motion assessment. The classical Haskell (1964) source model assumed the size l of instantly slipping zone on a fault to be much lower than complete fault length L . In similar relationship are local slip time, or rise time $T_r = l/v_r$, in which v_r is rupture velocity, and full rupture duration $T = L/v_r$. Heaton (1990) claimed the concept $l \ll L$ to be true on the basis of the results of several inversions of rupture space–time history and estimated $C_H = l/L = T_r/T$ to be on the order of 0.1. This was supported by later work (e.g., Somerville *et al.*, 1999). However, the accuracy of T_r estimates obtained in inversions was often limited. There are also certain doubts regarding the results of inversions in general (Razafindrakoto and Mai, 2014; Mai *et al.*, 2016) and of estimates of T_r in particular (Konca *et al.*, 2013; Somala *et al.*, 2014). Generally, most reliable T_r estimates may be expected from use of instruments located very near to the fault because such an instrument records the history of formation of static offset and therefore can give almost direct estimate of T_r . With increasing distance from a fault, quality of T_r estimates may be expected to deteriorate. With accumulation of many T_r estimates as components of descriptions of inversions stored in the SRCMOD database (Mai and Thingbaijam, 2014) and with mass determination of T_r from teleseismic

data (Melgar and Hayes, 2017), one can try to clarify whether these doubts are well grounded.

Data

The SRCMOD database stores data of inversions that used sets of various data. Table 1 contains T_r estimates extracted from SRCMOD only for cases when strong-motion data were used in an inversion. These estimates, denoted ATR (i.e., rise time, averaged over source elements), represent averages of T_r over elements of inverted source (subfaults). These numbers are accompanied by the value R_{\min} of fault distance of the strong-motion station closest to the fault. In a considerable fraction of cases, R_{\min} was lacking. In these cases, maps, tables, and texts of accessible original publications were examined, and often R_{\min} could be picked from these data at least approximately. Entries with unsettled R_{\min} or with zero T_r were rejected. In total, 73 entries were extracted from SRCMOD. About 10 more published source inversions were added to the data set (Table 2). In cases of several inversions for the same event, these were treated as independent entries; the number of events is 56. The 83 (M_w , T_r) pairs are shown in Figure 1. Data were split into two groups, with $R_{\min} \leq 5$ km and $R_{\min} > 5$ km. Linear regression was done; see Table 3 for parameters. Especially interesting is the log–log slope parameter β_r of the scaling relationship $T_r \propto M_0^{\beta_r}$. The match between estimates of the T_r versus M_0 trend for the two distance groups is unexpectedly good; β_r values are close, and absolute levels essentially match. Residual scatter is also similar. Initial expectations that use of records obtained at the smallest

*Also at Geophysical Survey, Kamchatka Branch, Russian Academy of Sciences, Petropavlovsk-Kamchatskii, Russia.

†Deceased (2018).

Table 1
Rise-Time Data Extracted from SRCMOD, with R_{\min} As Is or Revised

SRCMOD Tag	M_w	ATR	R_{\min}	SRCMOD Tag	M_w	ATR	R_{\min}
s1968TOKACH01NAGA	8.35	12	80	s1997KAGOSH01HORI	6.10	0.3	10
s1979COYOTE01LIUx	5.92	0.5	2	s1997KAGOSH02HORI	6.01	0.8	15
s1979IMPERI01ARCH	6.53	0.92	1	s1997KAGOSH01MIYA	6.04	0.75	10
s1979IMPERI01HART	6.58	0.7	3	s1997COLFIO01HERN	5.72	1.0	2
s1979IMPERI01OLSO	6.53	8.25	3	s1997COLFIO02HERN	5.97	1.0	3
s1987WHITTI01HART	5.89	0.4	2.5	s1997COLFIO03HERN	5.86	1.0	12
s1988SAGUEN01HART	5.81	0.5	43	s1998IWATEJ01NAKA	6.30	4.5	4
s1984NAGANO01TAKE	6.29	1.5	43	s1998IWATEJ01MIYA	6.27	7.5	4
s1984MORGAN01BERO	6.1	0.2	0.1	s1998HIDASW09IDEx	5.13	2.04	12
s1984MORGAN01HART	6.07	0.5	0.1	s1999CHICHI01MAxx	7.69	12	2
s1983BORAH01MEND	6.82	0.6	0	s1999CHICHI01SEKI	7.63	10.4	2
s1985MICH0A01MEND	8.01	6.0	18	s1999IZMITT01BOUC	7.59	3.25	20
s1985CENTRA01MEND	8.16	14	10	s1999IZMITT01SEKI	7.44	4.0	10
s1986NORTH01HART	6.21	0.4	4.6	s1999IZMITT01DELO	7.56	7.0	20
s1985NAHANN02HART	6.66	3	0	s1999IZMITT01YAGI	7.40	8.0	20
s1987SUPERS01WALD	6.51	1.5	0.7	s1999DUZCET01DELO	7.18	7.0	5
s1989LOMAPR01BERO	6.95	0.3	5.1	s1999DUZCET01BIRG	6.71	3.5	2
s1989LOMAPR01STEI	6.99	1.0	5	s1999OAXACA01HERN	7.47	1.92	17
s1989LOMAPR01WALD	6.94	1.9	5.1	s1999HECTOR01KAVE	7.24	13.2	27
s1991SIERRA01WALD	5.59	0.4	2	s1999HECTOR01JIxx	7.17	3.5	20
s1992LANDER01COHE	7.08	3.0	10	s2000TOTTOR01SEKI	6.83	3.5	5
s1992LANDER01COTT	7.29	3.13	1	s2000TOTTOR01IWAT	6.86	3.5	5
s1992LANDER01HERN	7.22	2.76	1	s2000TOTTOR01SEMM	6.73	1.24	1
s1992LANDER01WALD	7.28	6.0	12	s2002DENALI01OGLE	7.91	7.0	5
s1993HOKKAI01MEND	7.7	9.6	5	s2002DENALI01ASAN	7.87	7.0	5
s1994NORTH01WALD	6.80	1.4	1	s2003BOUMER01SEMM	7.25	1.33	20
s1994NORTH01HART	6.73	1.4	2	s2003TOKACH01KOKE	8.21	15.0	50
s1995KOBEDA01YOSH	6.86	3.0	34	s2003COLIMA01YAGI	7.50	13.0	120
s1995KOBEDA02SEKI	7.02	3.4	0.2	s2003MIYAGI01HIKI	6.10	4.0	30
s1995KOBEDA01KOKE	6.87	3.0	34	s2004NIIGAT01ASAN	6.62	3.5	2
s1995KOBEDA01IDEx	6.89	7.2	1	s2004PARKFI01CUST	6.06	0.88	1
s1995KOBEDA01HORI	7.01	3.0	5	s2005FUKUOK01ASAN	6.64	3.5	20
s1995KOBEDA01CHOx	6.80	3.0	5	s2008IWATEx01ASAN	6.89	4.5	3
s1995KOBEDA01WALD	6.92	2.7	1	s2011FUKUSH01TANA	6.68	3.5	15
s1996HYUGAx02YAGI	6.68	4.8	15	s2016KUMAMO02ASAN	7.04	5.0	2
s1996HYUGAx01YAGI	6.81	6.4	20	s2016KUMAMO01ASAN	6.14	3.0	3
s1997YAMAGU01MIYA	5.82	0.75	15				

ATR, rise time, averaged over source elements; R_{\min} , minimum distance between source and strong-motion station; SRCMOD Tag, event and publication tag for accessing SRCMOD entry. Bold italic values are the R_{\min} data added using maps and texts of original publications.

Table 2

Rise-Time Data Extracted from Original Publications

Event	M_w	ATR	R_{\min}	Reference
1966 Parkfield	5.6	0.3	0.1	Bouchon (1979)
1999 Chi Chi	7.7	7.00	1	Ji <i>et al.</i> (2003)
2003 San Simeone	6.6	2	15	Rolandone <i>et al.</i> (2006)
2009 L'Aquila	6.1	1.8	9	Cirella <i>et al.</i> (2012)
2009 L'Aquila	6.3	0.8	8	Poiata <i>et al.</i> (2012)
2014 South Napa	6	0.64	5	Ji <i>et al.</i> (2015)
2015 Gorkha	7.8	5.5	12	Avouac <i>et al.</i> (2015)
2015 Lefkada	6.6	2	10	Avallone <i>et al.</i> (2017)
2016 Amatrice	6.2	1.2	8	Tinti <i>et al.</i> (2016)
2016 Norcia	6.2	0.8	6	Liu <i>et al.</i> (2017)

possible distance from the ruptured surface makes some advantage did not show themselves, at least in the level of scatter. Evidently by coincidence, the fit of the slope of

the average β_r to the ideal $\beta_r = 1/3$ expected in the case of self-similarity is near to perfect, and real accuracy of β_r is probably on the order of 15%.

Discussion

Earlier estimates of the same trend (Somerville *et al.*, 1999; Miyake *et al.*, 2003) show similar β_r but markedly lower absolute levels. This difference is of practical significance because the value of T_r must be closely related to such parameters of strong motion as durations and periods of “forward directivity pulse” (Somerville *et al.*, 1997) and of “fling” (Bolt and Abrahamson, 2003). Among 15 data used in (Somerville *et al.*, 1999), 13 are obtained with the use of local data, with $R_{\min} < 10$ km. These points are marked on the plot but did not participate in regression. Points are not accurately overlapping with values from SRCMOD for the

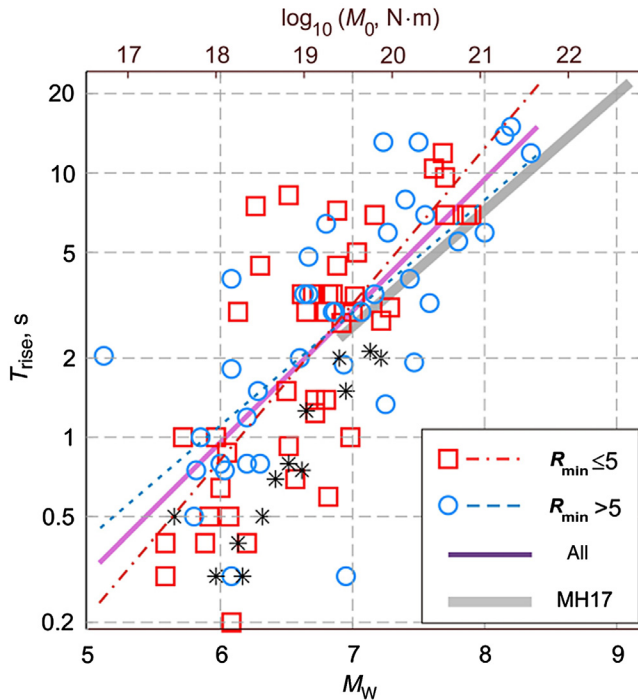


Figure 1. Rise time T_r estimates obtained with use of local data, plotted against M_w . Data are given separately for cases when the nearest strong-motion instrument was located at distance $R_{\min} > 5$ km from a fault or for cases of larger R_{\min} . Linear fits are shown for each group and for all data. For comparison, linear fit of teleseismic estimates after Melgar and Hayes (2017) is also reproduced. For comparison, the (M_w, T_r) pairs from Somerville *et al.* (1999) are also depicted when near-source data were used (asterisks). MH17, Melgar and Hayes (2017). The color version of this figure is available only in the electronic edition.

same inversions because of certain mismatch of accepted values of both M_w and T_r . These points are systematically located in the lower part of the data cloud. Among the 13 events in question, in two cases, many parallel inversions are present in SRCMOD. In both cases, the estimate used by Somerville *et al.* (1999) was the lowermost. The causes of the revealed systematic difference are not quite clear. The estimate of T_r obtained during inversion is often not quite certain. Reading the detailed descriptions of inversion procedures for the 13 cases, one can note that some authors

considered two parallel estimates of T_r , one with lower T_r and with lower total source M_0 and another with larger T_r and larger M_0 , better compatible with low-frequency teleseismic M_0 estimate. This suggests the role of probable expressed asymmetric profile of a slip pulse, with sharp initial spike and much longer trailing edge, as found by Guatteri *et al.* (2004). To describe such pulse shape, they introduce two separate time parameters, one that specifies the duration of initial spike and another for the duration of the tail part. If real slip pulses follow such pattern, this can easily lead to systematic misfit between results obtained by researchers having different attitudes. It seems that the approach to inversion used in earlier publications of 1988–1996 and in their compilation in (Somerville *et al.*, 1999) was slightly different than one used in the later ones, and somewhat lower estimates were preferable. Such an approach is completely justified because the derivation of the average T_r versus M_0 trend in Somerville *et al.* (1999) was specifically aimed at determination of expected periods of near-fault “forward directivity” velocity pulse and of near-fault acceleration spike related to “fling.” For this goal, the shorter of the two characteristic times of slip pulse is evidently preferable. Indeed, slip pulse, that is, slip velocity time function, must be differentiated once to get velocity or twice to get acceleration. The effect of the hypothetical longer characteristic time will be almost completely suppressed by these operations. Therefore, the absolute estimates of T_r based on the modern trend with average $C_H = 0.15$ – 0.18 probably need to be scaled down two to three times if used for prediction of characteristic period of “forward-directivity” velocity pulse or of near-fault acceleration peak.

Teleseismic estimates of the T_r versus M_0 trend obtained by Melgar and Hayes (2017) include 153 values for the M_w range 6.8–9.1. As for absolute level, these are in quite good match with those obtained using local data. The estimate of β_r equals 0.293, somewhat lower than 1/3 expected for the ideal “self-similarity scaling.” Melgar and Hayes (2017) also estimated the trend for source pulse length l ; in this case, individual variations of rupture velocity were taken into account. In this mode of analysis, they found $l \propto M_0^{0.268}$, therefore, the deviation from “self-similarity scaling” is even larger in this case. One might think that these

Table 3

Parameters of Linear Fit of $\log T_r$ versus M_w Relationship

Data Source	Data Volume	M_w Range	b	a	σ	β_r	T_r , s, at $M_w = 7$	C_H , at $M_w = 7$
SRCMOD, $R_{\min} \leq 5$ km	44	5–8	0.590	−3.63	0.320	0.393	3.0	0.17
SRCMOD, $R_{\min} > 5$ km	39	5–8.5	0.429	−2.53	0.315	0.286	2.9	0.16
SRCMOD, all data	83	5–8.5	0.498	−3.01	0.315	0.332	2.9	0.16
Heaton (1990)	7	5–7						0.1
Somerville <i>et al.</i> (1999)	15	5.6–7.3	1/2	−3.34	≈ 0.2	1/3	1.45	0.08
Miyake <i>et al.</i> (2003)	14	4.7–7	1/2	−3.34	≈ 0.1	1/3	1.45	0.08
Melgar and Hayes (2017)	153	6.8–9.1	0.439	−2.66	≈ 0.15	0.293	2.6	0.15

Approximating trend for $T_r(M_w)$ is $\log_{10}(T_r) = a + bM_w$; $\beta_r = b/1.5$; σ is standard deviation of residuals. $C_H = T_r/T \approx l/L$, approximate value assuming $v_r = 2.5$ km/s and $L(M_w = 7) = 45$ km.

deviations result from the fact that the full scale of M_w in the Melgar and Hayes (2017) data includes the range $M_w = 7.5\text{--}9$, in which the $M_0(L)$ scaling is known to deviate from self-similarity assumption even for subduction earthquakes (Scholz, 1982), probably because of limited fault width. This suggests, however, slower M_0 versus L trend, or, oppositely, steeper L versus M_0 trend, and this matches the Melgar and Hayes (2017) estimated trend of $L \propto M_0^{0.385}$. Therefore, no compensation arises: oppositely, the mentioned deviation of self-similarity for L is against such deviation for l . Dividing $l(M_0)$ and $L(M_0)$ trends, one obtains $C_H = l/L \propto M_0^{-0.117}$. This effect is quite noticeable. Assume $C_H = 0.17$ at $M_w = 7$ (Table 3); at $M_w = 9$, this would give $C_H = 0.17 \times 0.446 = 0.076$. Below $M_w = 7.5\text{--}8$, such effects may be less significant, and the “self-similarity behavior” seen in Figure 1 need not be put under doubt.

The well-established near-self-similarity scaling of T_r is in contradiction with the textbook concept that the second corner frequency of earthquake source spectrum f_{c2} is defined by T_r , so that $f_{c2} \propto 1/T_r$. Indeed, if this were true, the observed scaling of T_r would manifest itself as the trend of about $f_{c2} \propto M_0^{-0.3333}$. The actual f_{c2} versus M_0 trend is much more gradual (Gusev, 1983) and close to $f_{c2} \propto M_0^{-(0.17-0.20)}$ in the $M_w = 5\text{--}7.5$ range (Gusev, 2013; Denolle and Shearer, 2016) or even saturates at larger magnitudes (Denolle and Shearer, 2016). The revealed discrepancy is remarkable and needs separate analysis.

Conclusions

The main conclusions are as follows. First, both for local and teleseismic data, the slope of the rise time versus M_0 relationship $\beta_r = \frac{d \log T_r}{d \log M_0} \approx \frac{d \log l}{d \log M_0}$ does not deviate much from the value of 1/3 expected for the case of “self-similarity scaling.” The absolute value of the ratio $C_H = l/L$ is close to 1/6 at $M_w = 7$. The rise-time self-similarity is in contradiction with the fact that second corner frequency is defined by T_r because the actual f_{c2} versus M_0 trend is much more gradual. This implies that f_{c2} cannot be explained by the slip-pulse character of the rupture. Second, there is remarkable difference between absolute levels of the two groups of T_r estimates—the earlier (Somerville *et al.*, 1999) and the more recent. Its most probable cause is the different attitudes of researchers in the situation of probably rather asymmetric profile of slip pulse. The T_r values obtained in inversions of source evolution based on local or teleseismic data may significantly overestimate characteristic times related to near-source high-frequency strong motion.

Data and Resources

Data on finite earthquake source inversions were used as stored in the SRCMOD database: <http://equake-rc.info/srcmod> (last accessed July 2018). Other data used in this article came from published sources listed in the references.

Acknowledgments

The study was partly supported by the Russian Ministry of Education and Science under Grant Number 14.W03.31.003. The author is grateful to Valentina Zubova for technical assistance.

Publication of this article honors the author Alexander Gusev (1945–2018), who was the head of the Seismology Laboratory at the Institute of Volcanology and Seismology of the Far Eastern Branch of the Russian Academy of Sciences (RAS), and chief researcher at the Kamchatka Branch of Geophysical Survey of RAS. He graduated from the Department of Physics of the Moscow State University and moved to Kamchatka, which would become the focus of his professional interests. His main research areas were the earthquake source and its tectonophysical nature; fractal properties of seismic and volcanic processes, signals, and fields; engineering seismology; absorption and dispersion of seismic waves; and precursor detection. Publication of this final article is a fitting acknowledgment for a wonderful person, an outstanding seismologist, and an exceptional leader, known for his extensive knowledge, pedagogical talent, and the ability to captivate others with his ideas. Alexander A. Gusev passed away on 21 September 2018, shortly after finishing and submitting this article. Danila Chebrov (Kamchatka Branch of Geophysical Survey of RAS, Piip Boulevard 9, Petropavlovsk-Kamchatsky 683006, Russia; danila@emsd.ru) made minor revisions to this article.

References

- Avallone, A., A. Cirella, D. Cheloni, C. Tolomei, N. Theodoulidis, A. Piatanesi, P. Briole, and A. Ganas (2017). Near-source high-rate GPS, strong motion and InSAR observations to image the 2015 Lefkada (Greece) earthquake rupture history, *Sci. Rep.* **7**, Article Number 10358.
- Avouac, J. P., L. Meng, S. Wei, T. Wang, and J. P. Ampuero (2015). Lower edge of locked Main Himalayan thrust unzipped by the 2015 Gorkha earthquake, *Nature Geosci.* **8**, no. 9, 708.
- Bolt, B. A., and N. A. Abrahamson (2003). Estimation of strong seismic ground motions, in *International Handbook of Earthquake and Engineering Seismology*, W. H. K. Lee, H. Kanamori, P. C. Jennings, and C. Kisslinger (Editors), Vol. 81B, Academic Press, San Diego, California, 983–1001.
- Bouchon, M. (1979). Predictability of ground displacement and velocity near an earthquake fault: An example of the Parkfield earthquake of 1966, *J. Geophys. Res.* **84**, 6149–6156.
- Cirella, A., A. Piatanesi, E. Tinti, M. Chini, and M. Cocco (2012). Complexity of the rupture process during the 2009 L'Aquila, Italy, earthquake, *Geophys. J. Int.* **190**, 607–621.
- Denolle, M. A., and P. M. Shearer (2016). New perspectives on self-similarity for shallow thrust earthquakes, *J. Geophys. Res.* **121**, 6533–6565.
- Guatteri, M., P. M. Mai, and G. C. Beroza (2004). A pseudo-dynamic approximation to dynamic rupture models for strong ground motion prediction, *Bull. Seismol. Soc. Am.* **94**, 2051–2063.
- Gusev, A. A. (1983). Descriptive stochastic model of earthquake source radiation and its application to an estimation of short-period strong motion, *Geophys. J. Roy. Astron. Soc.* **74**, 787–808.
- Gusev, A. A. (2013). High-frequency radiation from an earthquake fault: A review and a hypothesis of fractal rupture front geometry, *Pure Appl. Geophys.* **170**, 65–93, doi: [10.1007/s00024-012-0455-y](https://doi.org/10.1007/s00024-012-0455-y).
- Haskell, N. A. (1964). Total energy and energy spectral density of elastic wave radiation from propagating faults, *Bull. Seismol. Soc. Am.* **54**, 1811–1841.
- Heaton, T. H. (1990). Evidence for and implications of self-healing pulses of slip in earthquake rupture, *Phys. Earth Planet. In.* **64**, 1–20.
- Ji, C., R. J. Archuleta, and C. Twardzik (2015). Rupture history of 2014 M_w 6.0 South Napa earthquake inferred from near-fault strong motion data and its impact to the practice of ground strong motion prediction, *Geophys. Res. Lett.* **42**, 2149–2156, doi: [10.1002/2015GL063335](https://doi.org/10.1002/2015GL063335).

- Ji, C., D. V. Helmberger, D. J. Wald, and K. F. Ma (2003). Slip history and dynamic implications of the 1999 Chi-Chi, Taiwan, earthquake, *J. Geophys. Res.* **108**, 2412, doi: [10.1029/2002JB001764](https://doi.org/10.1029/2002JB001764).
- Konca, A. O., Y. Kaneko, N. Lapusta, and J. P. Avouac (2013). Kinematic inversion of physically plausible earthquake source models obtained from dynamic rupture simulations, *Bull. Seismol. Soc. Am.* **103**, 2621–2644, doi: [10.1785/0120120358](https://doi.org/10.1785/0120120358).
- Liu, C., Y. Zheng, Z. Xie, and X. Xiong (2017). Rupture features of the 2016 M_w 6.2 Norcia earthquake and its possible relationship with strong seismic hazards, *Geophys. Res. Lett.* **44**, 1320–1328, doi: [10.1002/2016GL071958](https://doi.org/10.1002/2016GL071958).
- Mai, P. M., and K. K. S. Thingbaijam (2014). SRCMOD: An online database of finite-fault rupture models, *Seismol. Res. Lett.* **85**, 1348–1357.
- Mai, P. M., D. Schorlemmer, M. Page, J.-P. Ampuero, K. Asano, M. Causse, S. Custodio, W. Fan, G. Festa, M. Galis, *et al.* (2016). The earthquake-source inversion validation (SIV) project, *Seismol. Res. Lett.* **87**, 690–708.
- Melgar, D., and G. P. Hayes (2017). Systematic observations of the slip pulse properties of large earthquake ruptures, *Geophys. Res. Lett.* **44**, 9691–9698.
- Miyake, H., T. Iwata, and K. Irikura (2003). Source characterization for broadband ground-motion simulation: Kinematic heterogeneous source model and strong motion generation area, *Bull. Seismol. Soc. Am.* **93**, 2531–2545.
- Poiata, N., K. Koketsu, A. Vuan, and H. Miyake (2012). Low-frequency and broad-band source models for the 2009 L'Aquila, Italy, earthquake, *Geophys. J. Int.* **191**, 224–242.
- Razafindrakoto, H. N., and P. M. Mai (2014). Uncertainty in earthquake source imaging due to variations in source time function and earth structure, *Bull. Seismol. Soc. Am.* **104**, 855–874.
- Rolandone, F., D. Dreger, M. Murray, and R. Bürgmann (2006). Coseismic slip distribution of the 2003 M_w 6.6 San Simeon earthquake, California, determined from GPS measurements and seismic waveform data, *Geophys. Res. Lett.* **33**, no. 16, doi: [10.1029/2006GL027079](https://doi.org/10.1029/2006GL027079).
- Scholz, C. H. (1982). Scaling laws for large earthquakes: Consequences for physical models, *Bull. Seismol. Soc. Am.* **72**, 1–14.
- Somala, S. N., J. P. Ampuero, and N. Lapusta (2014). Resolution of rise time in earthquake slip inversions: Effect of station spacing and rupture velocity, *Bull. Seismol. Soc. Am.* **104**, 2717–2734.
- Somerville, P. G., K. Irikura, R. Graves, S. Sawada, D. Wald, N. Abrahamson, Y. Iwasaki, T. Kagawa, N. Smith, and A. Kowada (1999). Characterizing earthquake slip models for the prediction of strong ground motion, *Seismol. Res. Lett.* **70**, 59–80.
- Somerville, P. G., N. F. Smith, R. W. Graves, and N. A. Abrahamson (1997). Modification of empirical strong ground motion attenuation relations to include the amplitude and duration effects of rupture directivity, *Seismol. Res. Lett.* **68**, 199–222.
- Tinti, E., L. Scognamiglio, A. Michelini, and M. Cocco (2016). Slip heterogeneity and directivity of the M_L 6.0, 2016, Amatrice earthquake estimated with rapid finite-fault inversion, *Geophys. Res. Lett.* **43**, 10,745–10,752.

Alexander A. Gusev

Institute of Volcanology and Seismology
Far East Branch
Russian Academy of Sciences
9 Piip Boulevard
Petropavlosk-Kamchatsky 683006, Russia
gusev@emsd.ru

Danila Chebrov

Kamchatka Branch of Geophysical Survey of Russian Academy of Science
9 Piip Boulevard
Petropavlovsk-Kamchatsky 683006, Russia
danila@emsd.ru

Manuscript received 5 August 2018;

Published Online 1 October 2019